EFFECT OF RARE EARTH ADDITIONS ON GRAIN REFINEMENT OF PLAIN CARBON STEELS

R. Tuttle
Department of Mechanical Engineering, Saginaw Valley State University, University Center, MI, USA

Abstract

This paper describes a set of experiments with misch metal and rare earth silicide additions in 1010 and 1030 steel to determine whether grain refinement occurs. Target rare earth (RE) contents of 0.1 and 0.2% were employed. After melting, the desired RE addition was added during tapping and then poured into green sand molds. The resulting test plates were then sectioned for tensile and metallographic testing. Yield strength increased for several of the 1010 and 1030 samples. The increase in yield strength correlated with a reduction in grain size. A dramatic increase in percent elongation was also observed in the 1010 sample with the smallest grain size. Electron microscopy found complex RE oxides. These oxides appear to act as heterogeneous nuclei. When they were coated with another slag, the grain size and mechanical properties were similar to the baseline material in both the 1010 and 1030.

Keywords: *steel, grain refinement, 1010, 1030, rare earth, misch metal, rare earth silicide*

Introduction

Over the past decade, there have been significant advancements in the steels produced by steel mills. These new steels provide higher levels of strength through multi-phase microstructures. Specialized thermomechanical processing routes and alloy additions cause the increased strength in most of these alloys. Steel foundries cannot use thermomechanical processing routes to increase the strength of their steels. As a result, the advanced steels developed by the wrought steel industry have not been as successful for foundries. The net result is that the steel foundry industry must develop methods of strengthening steel that are effective in their manufacturing process.

One possible route for improving the strength of cast steels is to reduce the grain size. Decreasing the grain size increases the number of grain boundaries which impedes dislocation motion within the metal crystal. Decreasing the grain size during solidification requires the introduction of a significant number of heterogeneous nuclei. A large number of heterogeneous nuclei allow a multitude of steel grains to grow. These more populous steel grains continue to grow in the liquid until they impinge on each other. Since there are more steel grains, impingement occurs sooner than when fewer nuclei are present, providing the resulting reduction in grain size. Grain refinement has been successfully employed in aluminum, magnesium, and copper alloys as a viable foundry technology.[1-3]

The basis of solidification based grain refinement is the manipulation of the number of grains nucleated through heterogeneous nucleation events. This requires the introduction of heterogeneous nuclei into the melt. These nuclei must meet four criteria: be solid at the liquidus temperature of the melt; be thermodynamically stable in the melt; be wetted by the melt; and have a similar crystallographic structure.[1,4,5] Reference data for prospective nucleating phases can readily identify compounds that are solid at the melt's liquidus temperature. Thermodynamic data can be evaluated by Gibbs' free energy minimization methods. These determine the stability of a candidate nucleation compound in a melt through computerized methods. Wetting data for liquid metal systems is difficult to obtain and frequently unavailable when selecting candidate phases.[2,4] Crystallographic similarity between the candidate nucleation compound and the solid phase of the melt can be determined using reference crystallographic data and the following equation:

$$\delta^{(hkl)_s}_{(hkl)_n} = \sum_{i=1}^{3} \frac{\left|\left(d^{i}_{[uvw]_s}\cos\theta\right) - d^{i}_{[uvw]_n}\right|}{d^{i}_{[uvw]_n}} * 100 \qquad \text{Eqn. 1}$$

where $(hkl)_s$ is a low-index plane of the substrate, $[uvw]_s$ is a low-index direction in $(hkl)_s$, $(hkl)_n$ is a low-index plane in the nucleated solid, $[uvw]_n$ is a low-index direction in $(hkl)_n$, $d_{[uvw]n}$ is the interatomic spacing along $[uvw]_n$, $d_{[uvw]s}$ is the interatomic spacing along $[uvw]_s$, and θ is the angle between the $[uvw]_s$ and $[uvw]_n$. Equation 1 is the Generalized Turnbull-Vonnegut equation which provides the ability to determine the average difference between atom positions on the crystallographic planes of two crystal structures.[5] The result is a determination of the lattice disregistry, or difference in lattice parameters, between two phases. Experimental evi-

dence has shown that, when the lattice disregistry is small at the melting point of the melt, the solid phase can nucleate the other solid.[1-5] In the case of steel, this means a proposed nucleation compound would assist the nucleation of either δ-ferrite or austenite.

Several authors have reported a reduction in grain size due to the addition of rare earth (RE) elements.[6-12] Much of the work employing RE additions has been in austenitic stainless steels.[8,9,11] Some research has been done in plain carbon steels.[7,10] In terms of actual mechanical properties due to the refinement, minimal information exists.

J.J. Moore made the earliest reference to RE additions reducing grain size.[6] The focus of his work was to desulfurize sand cast steels to improve impact toughness. He produced a 0.10%C, 1.25%Mn steel which was poured into cylindrical resin-bonded sand molds. Both misch metal and RE silicide additions were examined. The types of inclusions were characterized. The author reported complex RE-Al-Mn-O-S oxysulphides as the predominant inclusion type. The sulfur level in the steel matrix was reduced by 90%. The sulfur was found to be tied up in the complex oxysulphides.[6] Moore noticed a reduction in grain size, but attributed the improvement in properties to a reduction in sulfur content in the steel matrix.[6]

Li et al. conducted two series of experiments on 1045 steel with RE additions.[7] The first set of experiments measured the cooling curve of solidifying ingots. Rare earth additions were accomplished by adding RE silicide and CeO_2 powder. The CeO_2 powder was theorized to be capable of acting as a heterogeneous nuclei. Rare earth addition levels of 0.10%, 0.16%, and 0.40% were examined. Li et al. measured a reduction in primary dendrite arm spacing and secondary dendrite arm spacing (SDAS) with RE additions placed in the ingot mold. Rare earth additions added in the furnace had no effect on the microstructure of the steel.[7] The authors further reported the addition of CeO_2 had no effect on primary dendrite arm spacing or SDAS. The second series of experiments focused on the degree of undercooling required for nucleation and surface tension change. This second series consisted of a levitation drop experiment on 1045 steel with the same additions as the ingot experiment. The addition of both CeO_2 and RE decreased the undercooling required to initiate solidification. Li et al. also measured a reduction in the surface tension in the droplets. Moreover, they observed a single crystal rim on the solidified droplets. The cause of this single crystal rim was attributed to the high cooling rate and steep temperature gradient at the exterior of the droplet. They concluded RE silicide additions reduced the grain size and undercooling for solidification; however, evidence to prove that CeO_2 assisted with nucleation was insufficient. The authors theory was cerium redistribution during solidification impeded dendrite growth, which resulted in the observed SDAS and undercooling decrease.

Eijk and Walmsey experimented with RE additions in super austenitic stainless steel.[8] A heat of the super austenitic stainless steel was melted at an industrial steel mill. An iron-chromium-cerium master alloy was added at a rate of 3.5 kg per ton into a ladle. The ladle was then poured into a cast iron ingot mold to solidify. Next, the ingot was sectioned and metallographically examined. Eijk and Walmsey observed the SDAS dramatically decreased in the heat containing the iron-chromium-cerium addition. The authors stated that several different cerium and aluminum oxides were observed in the cerium treated ingot. Transmission electron microscopy examination of the cerium treated ingot found several $AlCeO_3$ inclusions that had excellent alignment with the surrounding austenitic matrix. The authors concluded these particles served as heterogeneous nuclei since their lattice parameter was only 3.82% larger than that of the surrounding austenite.

Suito and co-workers examined the role Ce_2O_3, ZrO_2, and MgO particles played in determining the structure of steels.[9] Several 70 g, 10%Ni steel heats were melted in an induction furnace. Either titanium, zirconium, or cerium was added to deoxidize the melt and form the desired oxide inclusions. A series of 0.15 to 0.50%C steels were created in 70 g heat sizes to determine the role of oxide particles in affecting the grain size of these alloys. For each carbon level experimented with, either aluminum, titanium, zirconium, or cerium was added with either calcium or magnesium to deoxidize the melt and create specific oxide inclusions. After melting the 70 g sample in an alumina crucible, the melt was cooled to 1400ºC before being quenched to room temperature. The authors stated that for the 10%Ni samples, the area fraction of equiaxed grain increased in accordance with the lattice disregistry of the primary oxides formed.

In the case of the 0.15% to 0.50%C alloys, there was a reduction in grain size when Ce_2O_3, ZrO_2, and MgO particles were present. However, not all of these particles have a low lattice disregistry with austenite or -ferrite. Suito et al. theorized that Zener pinning was the dominant mechanism. Zener pinning occurs when an inclusion retards the growth of the solidifying phase during grain growth as the metal cools to room temperature. The authors thought Zener pinning was a more appropriate explanation since the decrease in grain size corresponded to the presence of a large number of inclusions in those samples.[9]

In work on a 0.20%C, 0.02%P steel, Guo et al. examined the role of Ce_2O_3 and CeS particles.[10] A 70 g sample was induction melted under an argon or argon-7 vol% H_2 atmosphere. Cerium metal was added to create Ce_2O_3 inclusions. In a second set of experiments, sulfur was added to the same steel by a Fe-36%S alloy addition. Cerium metal also was added to form CeS particles. The sample then was cooled from 1873K to 1673K at a cooling rate of 1.02 K/s. After solidifying, 0.3 g of the sample was dissolved away to isolate

the inclusions. These inclusions then were analyzed to determine of each inclusion's amount and the dissolved cerium content. Metallographic analysis of the samples found that primary dendrite arm spacing decreased with increasing cerium content. Dendrite arm spacing shrank with an increase in either cerium content or the amount of Ce_2O_3 and CeS particles.[10] The equiaxed grain area fraction increased with a rise in Ce_2O_3 or CeS inclusions, but it was unaffected by the soluble cerium content. The degree of undercooling for solidification decreased with larger amounts of Ce_2O_3 particles.[10] No mechanical properties were reported by Guo et al.

Lan and fellow researchers studied the effects of RE additions on H13 tool steel.[12] A 20 kg heat of H13 tool steel was prepared for each experimental treatment. The melt was deoxidized with aluminum and poured at 1873K into an investment casting mold preheated to 873K. Prior to pouring, misch metal was placed at the bottom of the downsprue in the mold. The solidified casting was normalized and then quenched and tempered to reduce segregation. Lan noted that microsegregation within the casting was significantly reduced for chromium, molybdenum, and vanadium. These authors also observed a reduction in the SDAS.[12] Unnotched impact testing was conducted on samples from the casting. The RE-containing samples had dramatically higher impact toughness than the reference H13 casting. This is despite similar hardnesses between the RE and non-RE samples.[12] These authors attributed the improvement in impact toughness on the reduction in SDAS. The SDAS reduction was thought to be caused by the presence of Ce_2O_3 particles acting as heterogeneous nuclei.[12]

There has been considerable debate in the literature on the role RE oxide inclusions play in decreasing grain size. Some authors theorize the particles act as heterogeneous nuclei, while others theorize the oxides pin the austenite grain boundaries and reduce grain growth. Many of the experiments have been conducted in small scale laboratory experiments that may not have reflected industrial conditions. Of the few studies done on RE additions in an industrial environment only one was done on carbon steels in a foundry environment.[6] Only one author reported mechanical properties; however, the focus was more on impact properties and removal of sulfur than strength.[6] No attempt was made to examine the improvements in properties as a function of grain size. To address these issues, the current paper investigated the role of RE additions on the structure and properties of 1010 and 1030 steel in the as-cast condition under conditions more closely replicating foundry practice. Rare earth additions were accomplished through a ladle addition of either misch metal or rare earth silicide. Rare earth levels of 0.1 and 0.2% were evaluated. Cast plates were poured from each alloy in green sand molds and sectioned for metallographic and tensile testing. An increase in tensile properties was observed for many of the RE samples. Percent elongation also dramatically improved in the 1010 material.

Experimental Procedure

A 23 kg heat of either 1010 or 1030 steel was melted in a 3 kHz induction furnace. Once the melt reached 1650ºC, carbon, ferro-manganese, and a small amount of aluminum was

Table 1. Chemical Analysis of Rare Earth Alloy Additions

Alloy	Total RE (%)	Ce (%)	La (%)	Si (%)	Al(%)	Ca (%)	Ti(%)	Fe (%)	Mg (%)
Misch Metal	99	70.5	29.3	-	-	-	-	0.2	0.4
RE silicide	31.5	17.1	Not specified	35.69	0.29	1.19	0.23	-	-

Table 2. Experimental Heat Chemical Analysis

Heat	C (%)	Si (%)	Mn (%)	P (%)	S(%)	Al (%)	Total RE (%)
1010	0.10	0.016	0.24	0.006	0.008	0.054	-
1010 -0.1% RS	0.10	0.17	0.26	0.007	0.010	0.196	0.081
1010 -0.2% RS	0.10	0.187	0.113	0.007	0.008	0.141	0.12
1010- 0.1% MM	0.08	0.015	0.086	0.008	0.007	0.097	0.0078
1010 -0.2% MM	0.13	0.014	0.22	0.010	0.007	0.164	0.044
1030	0.40	0.09	0.76	0.012	0.0053	0.085	-
1030 -0.1% RS	0.40	0.038	0.58	0.012	0.005	0.037	0.04
1030 -0.2% RS	0.33	0.122	0.464	0.009	0.005	0.161	0.099
1030 -0.1% MM	0.38	0.089	0.59	0.013	0.010	0.173	0.077
1030 -0.2% MM	0.39	0.048	0.64	.011	0.005	0.0710	0.333

added. The melt was tapped into a ladle at 1720ºC. The final aluminum deoxidation and RE additions were added. Rare earth additions were accomplished by either the addition of misch metal or RE silicide. The additions were added to the melt by placing them into the tapping stream when the ladle was approximately one-third full. Table 1 lists the chemical analysis of these two master alloys. For each RE addition type, two different target RE contents were used, 0.1% and 0.2%. Table 2 lists the chemistries for each heat. The heats listed with MM in the name had a misch metal addition; the heats with RS in the name had a RE silicide addition. To assist with heterogeneous nucleation -325 mesh chemically pure La_2O_3 powder was added to one mold poured from each heat chemistry. The powder was poured into the steel stream as it entered the downsprue of the mold. A target pouring temperature of 1620ºC was used for pouring the molds.

The test casting consisted of a plate casting, 2.51 cm thick, 12.7 cm wide, and 25 cm long, with a large riser (Figure 1). Green sand molds were made from AFS GFN 65 silica sand with a 1.7% calcium bentonite, 1.8% sodium bentonite clay content and 2.4% water content. A jolt/squeeze machine prepared the molds. After pouring, the molds cooled for one hour before shakeout. This resulted in a casting temperature below 535ºC at shakeout. Then, the casting continued to air cool to room temperature after shakeout.

Each plate was sectioned into 2.25 cm square, 12.7 cm long samples. One sample was metallographically examined and used for optical emission spectroscopy to verify the plate's chemical analysis. The remaining four bars were turned into 1.27 cm diameter tensile bars according to ASTM standard E8-04. Machining and tensile testing were completed by a local foundry with a servo-hydraulic mechanical testing frame with an extensometer.

The metallographic samples were prepared using standard metallographic techniques. A semi-automatic polisher ground and polished the samples. Polishing was accomplished with 6 µm and 1 µm polycrystalline diamond and a final polish of 0.05 µm alumina. A 3% nitol etch was employed. Electron microscopy was conducted on the metallographic and tensile bar fracture surfaces with an energy dispersive spectrometer (EDS) equipped scanning electron microscope (SEM). An accelerating voltage of 15 kV was used.

Results and Discussion

Gating System

Computer simulations of the gating system were carried out prior to casting production. The simulations examined the fluid flow and solidification of the test casting. No macroshrinkage or microshrinkage porosity was predicted within the region where tensile bars would be removed. The relatively large riser size assisted in creating directional solidification within the test section of the part. Fluid flow simulation results predicted low fluid flow velocities within the casting and the in-gate. A velocity profile line had been inserted into the simulation geometry to determine the velocity profile across the in-gate where it entered the casting at each simulation time step. Velocity peaked at 0.7943 seconds into filling and decreased after that. The highest velocity observed in the simulation results was 0.518 m/s (Figure

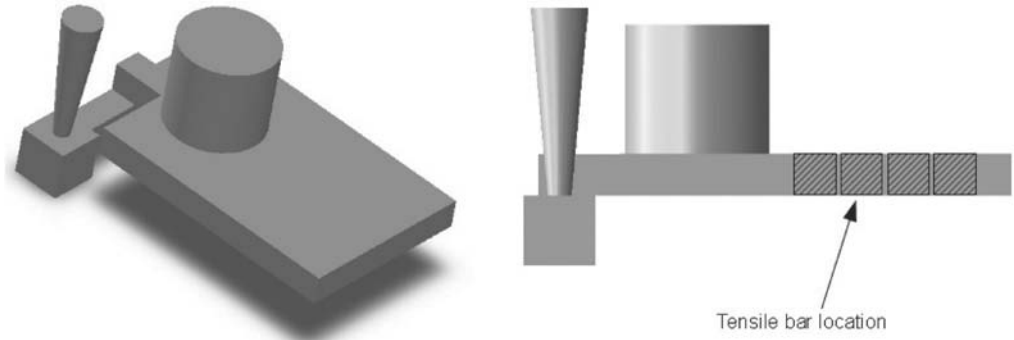

Figure 1. Illustration of test casting used.

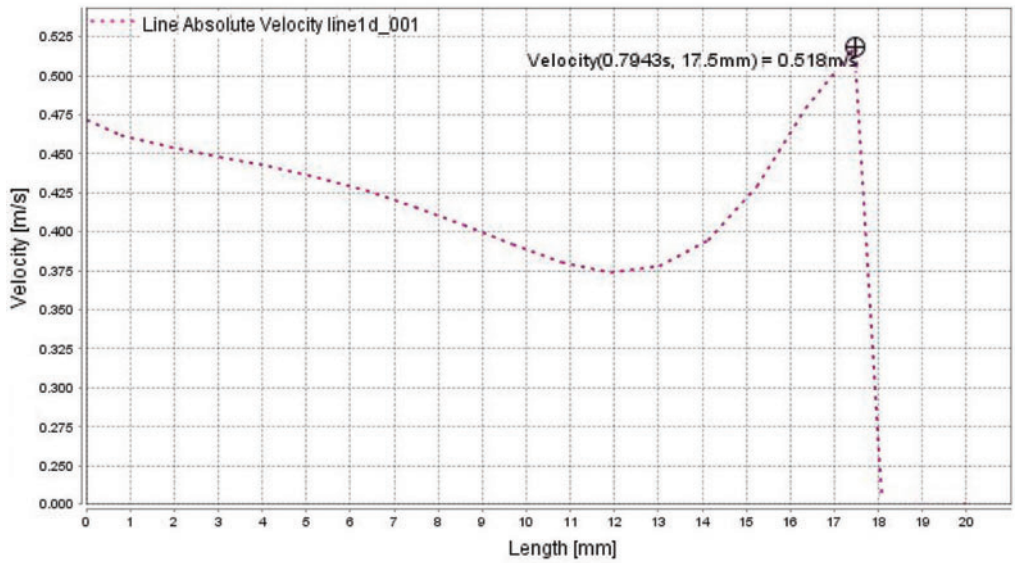

Figure 2. In-gate velocity predictions at 0.7943 seconds.

2). This is only slightly higher than the critical velocity of 0.5 m/s recommended by other researchers and within the prediction errors of the simulation.[13] The overall fluid flow was relatively laminar, and a uniform filling profile was maintained as the casting filled. A close examination of the fluid flow within the in-gate at the peak velocity reveals a laminar flow with little recirculation and no indication of turbulent flow (See Figure 3).

The laminar fluid flow within the casting and low fluid velocities would result in little reoxidation within the casting during filling. It would be possible for reoxidation products from ladle filling to enter the casting since no filter was utilized in the gating system; however, an unfiltered gating system had been intentionally employed so RE oxides that formed within the ladle during filling would not be removed. Removal of these oxides might completely prevent refinement.

Mechanical Testing

Figures 4 and 5 illustrate the yield strength (YS), ultimate tensile strength (UTS), and percent elongation (EL) for the 1010 tensile bars. No mechanical properties were reported for the 1010 heat with 0.1% misch metal and La_2O_3 additions. After pouring this casting four times, the author was unable to obtain a porosity free casting.

The yield strength of most of the RE addition samples was higher than the as-cast 1010 material. The average yield strength of the baseline as-cast 1010 was 170 MPa; the average yield strength of the 1010 with 0.1% rare earth silicide and La_2O_3 addition was 195 MPa. The UTS was similar between the baseline as-cast 1010 and all of the RE samples except the 1010 with 0.1% misch metal addition, which was lower. Elongation for some of the tensile bars was significantly higher than the baseline as-cast 1010. The best elongations were for the samples containing 0.2% misch metal addition and with 0.1% rare earth silicide and La_2O_3 addition. Of particular interest was the 1010 with 0.1% rare earth silicide and La_2O_3, two of the tensile bars had an elongation around 38% while the other two had an elongation of 8%. This large difference in tensile bar elongation is surprising. The same set of tensile bars had very similar yield strengths.

Figure 6 depicts the yield strength as a function of actual total rare earth content. At a total RE content of 0.007%, the yield strength of the bars was lower than the baseline as-cast 1010 material. Yield strength appears to peak around 0.04% and then gradually decline (Figure 6). However, even at 0.12% total rare earth (TRE), the strength is higher than the baseline as-cast 1010. It should be noted, at a TRE above 0.8%, the samples with La_2O_3 powder additions were stronger than the samples containing only a RE addition. It appears the La_2O_3 additions were only effective when sufficient RE was in the melt. The excess RE may restrict grain growth and increase constitutional un-

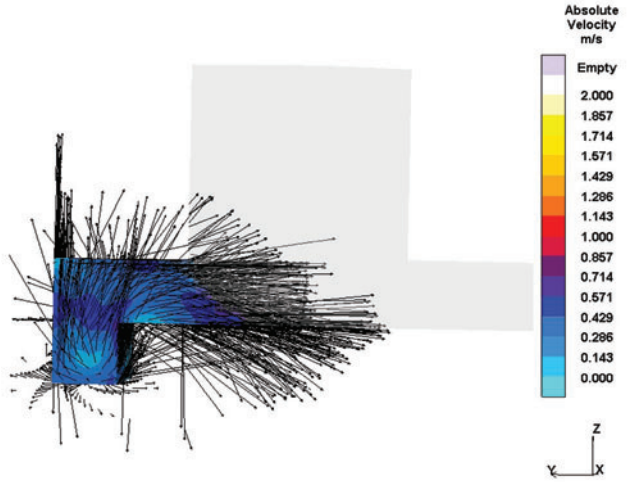

Figure 3. Velocity plot of the in-gate with velocity vectors depicting flow within the in-gate at 0.7943 seconds

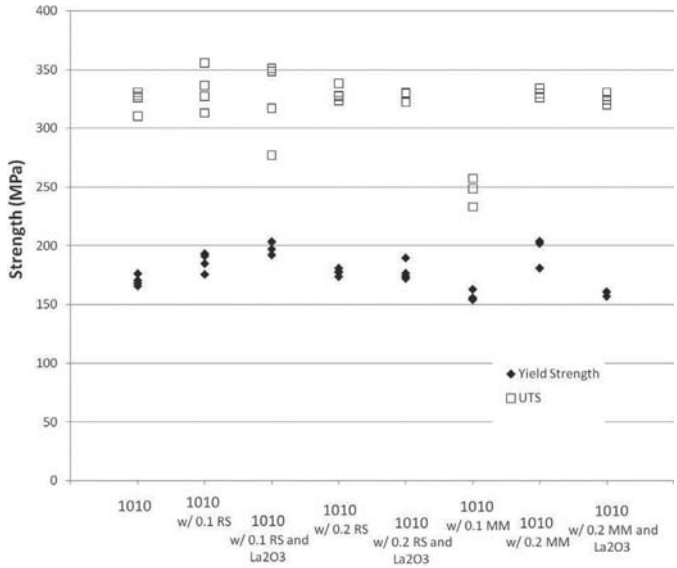

Figure 4. Yield strength and ultimate tensile strength of the 1010 bars.

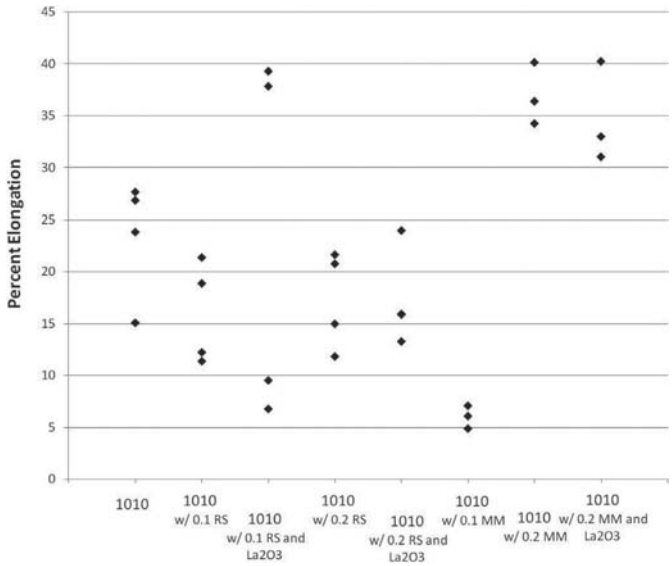

Figure 5. Percent elongation of 1010 tensile bars.

dercooling in the alloy, which enables the La_2O_3 particles to act as nucleation sites. The heats with RE silicide additions had the higher TRE levels in Figure 6. The likely cause of this higher recovery is the higher silicon content of the ferroalloy protecting the RE from oxidation prior to entering the steel.

There were several RE containing samples with yield strengths higher than the baseline as-cast 1030 heat (See Figure 7). The average yield strength for the baseline heat was 262 MPa. The average strength for the 1030 with 0.2% misch metal was 319 MPa. It is interesting to note that the 1030 with 0.2% RE silicide sample had a similar average yield strength and UTS to the baseline despite a significantly lower carbon level. Unlike the 1010 results, the UTS was lower for several samples. Two-thirds of the samples with low UTS contained a La_2O_3 powder addition. The elongation for the tensile bars showed no indication of a significant difference (See Figure 8).

Evaluating the strength as a function of TRE reveals behavior different from 1010 steel (Figure 9). Yield strength increased with the TRE content. The 1030 samples containing 0.099% TRE with 0.2% rare earth silicide had dramatically lower carbon content than the other samples. The lower carbon content would explain their significantly lower strength.

Optical Microscopy

Representative micrographs of the 1010 samples without La_2O_3 powder addition are illustrated in Figures 10-14.

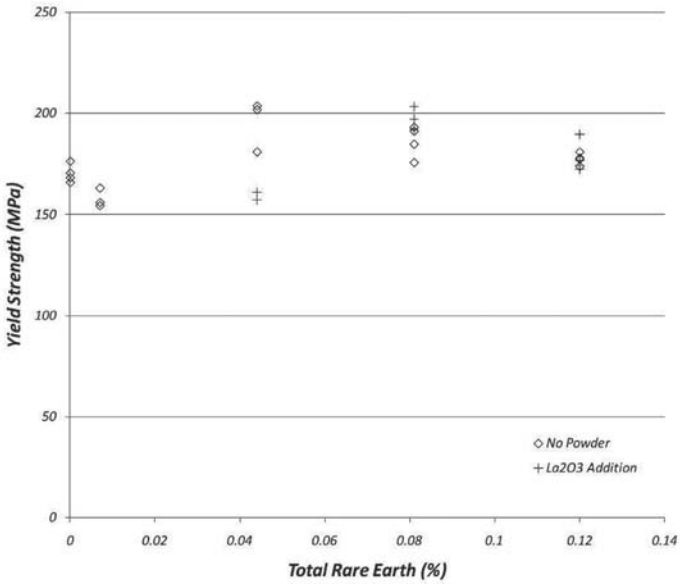

Figure 6. Yield strength verses the actual rare earth content of each 1010 tensile bar tested.

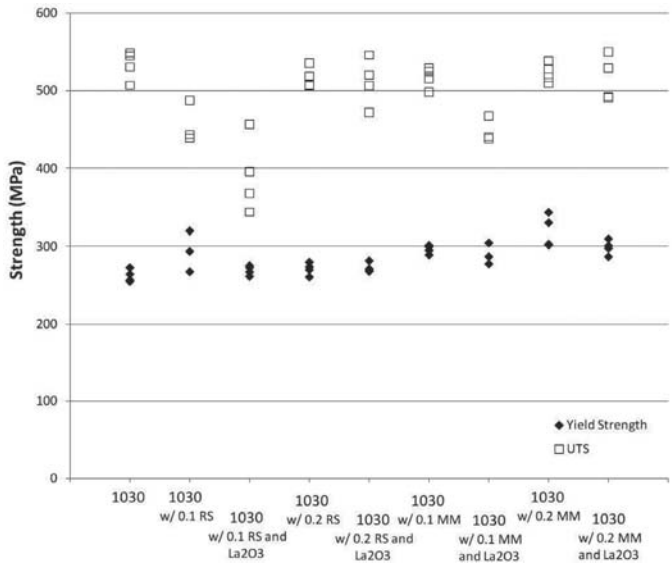

Figure 7. Yield strength and ultimate tensile strength for 1030 samples.

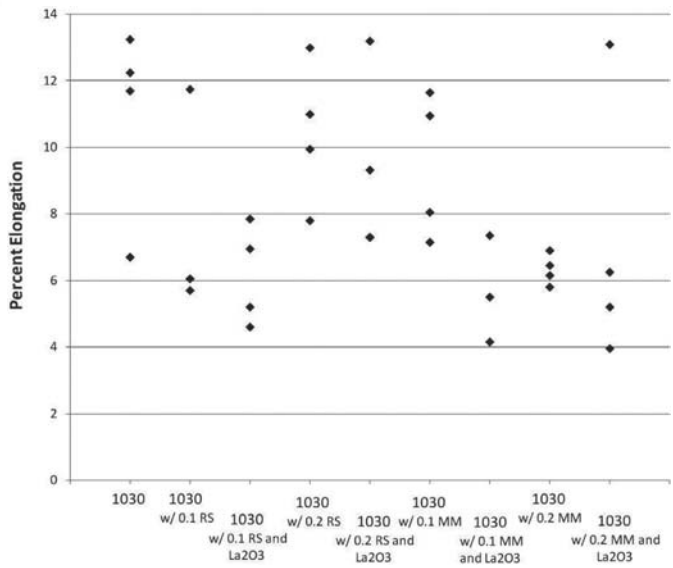

Figure 8. Percent elongation of the 1030 samples.

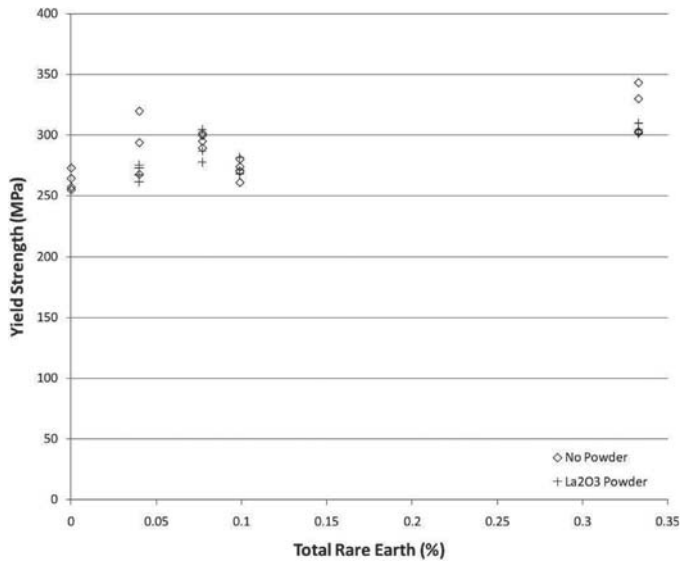

Figure 9. Yield strength as a function of TRE for the 1030 samples.

Only the no powder addition micrographs are presented since there was not a significant difference in structure. Grain size comparison between samples was done through visual inspection.

The 1010 samples with 0.1% RE silicide had a smaller overall grain size. This is consistent with the Hall-Petch grain size strengthening mechanism. A reduction in grain size produces an increase in strength. The grain size reduction could be due to the formation of RE_2O_3 type oxides.[8,9,10] Tensile data for this sample did find a higher yield strength than the baseline 1010 material.

The 1010 0.2% RE silicide sample had no evidence of grain refinement (Figure 12). Considering that this sample had an average yield strength of 177 MPa, the results are consistent with grain size being the dominant strengthening mechanism in the 1010 samples. The lack of refinement (despite this sample having the highest rare earth content) seems inconsistent with the formation of heterogeneous nuclei.

In the 1010 sample with 0.1% MM, the author observed several regions of large grains and smaller grains. This can be observed in Figure 13, where the center of the image contains several small grains and the upper left portion contains a larger grain. The large variation in grain size would indicate regions of high and low nuclei density. Regions with a low nuclei density developed larger grains. The cause of this may be related to the low TRE. During the ladle addition of the misch metal, the sample is exposed to oxygen from the atmosphere which can react to form RE oxides. The low TRE content indicates significant oxidation loss occurred. At such a high oxidation loss, it is likely "huge" oxides formed. The "huge" oxides would have a significant buoyancy force resulting in flotation. The oxides also could have formed on the melt surface. In either case, they would have become part of the ladle slag and not the melt. Some of the RE content could have also oxidized into small particles that were mixed into the melt and remained there during pouring. These smaller particles may have clumped near each other and produced a region of high nuclei density, which then developed a small grain size region in the casting.

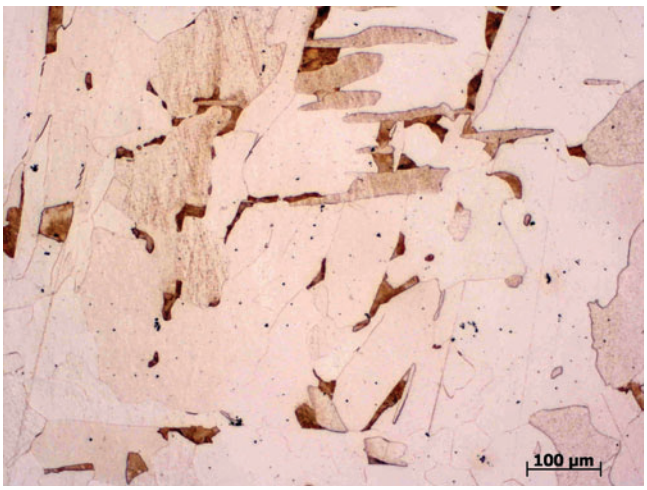

Figure 10. Micrograph of baseline as-cast 1010 sample.

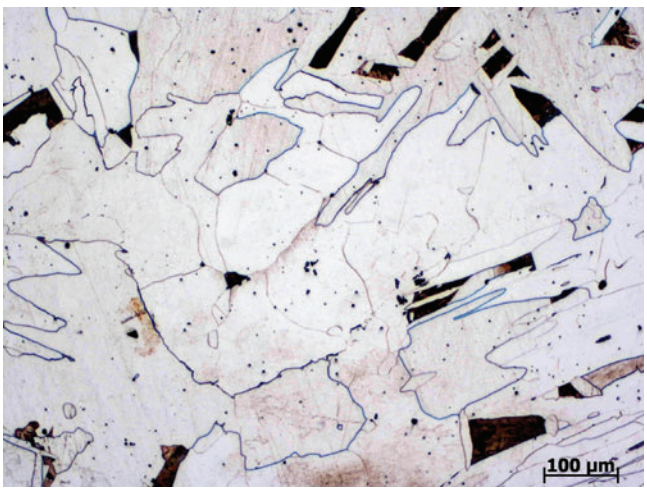

Figure 11. Micrograph of 1010 0.1% RS sample.

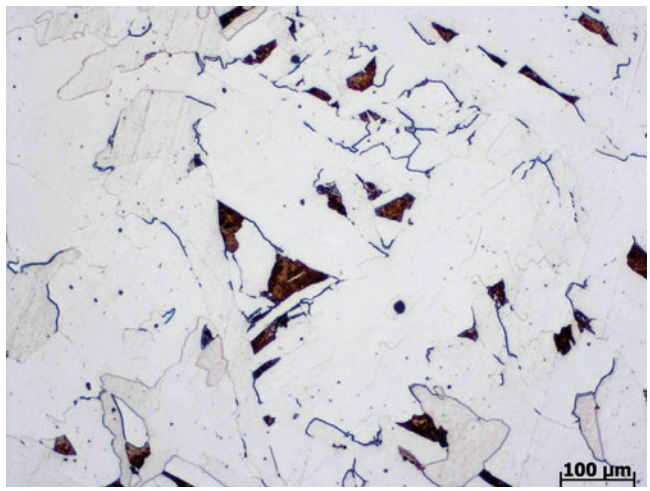

Figure 12. Micrograph of 1010 with 0.2% RS sample.

Figure 13. Micrograph of 1010 with 0.1% MM sample.

The 1010 steel with 0.2% misch metal addition had a higher yield strength and elongation than the baseline as-cast 1010. The average yield strength for these samples was 195 MPa, and the average percent elongation was 37%. It also had the finest structure of all the 1010 samples examined. The smaller grain size is consistent with the misch metal acting as a grain refiner. An improvement in elongation is consistent with reported findings in aluminum alloys that have been grain refined.[14,15]

Figures 15-19 are representative micrographs of the 1030 samples without a powder addition. Like the 1010 samples, the 1030 samples with a La_2O_3 powder addition were not significantly different enough to warrant inclusion.

The 1030 sample with 0.1% RE silicide had a finer structure than the baseline 1030 material. The free ferrite within the microstructure did not appear to be appreciably smaller than the baseline material. However, the distance between the free ferrite is less than the baseline 1030. The pearlite colony size decreased in these samples. Other researchers have found a decrease in pearlite colony size can increase strength.[16,17] This reduction in distance between adjoining free ferrite and smaller pearlite colony size strengthened the material. It is possible that both are caused by a reduction in the prior austenite grain size through heterogeneous nucleation. However, it is also plausible the rare earth elements affected carbon diffusion during the eutectoid reaction and created the observed structure. This had been found with other alloying elements in steel.[16] Evidence in the optical microscopy and tensile testing results is insufficient to develop a definitive conclusion.

The structure of the 1030 steel with 0.2% RE silicide was similar to that of the baseline 1030 sample (Figure 17). This is consistent with a grain or pearlite colony size dominant strengthening mechanism since the two materials had similar mechanical properties. It should be noted, while this sample had a higher RE content than the 0.1% RE silicide and 0.1% misch metal sample, refinement did not occur.

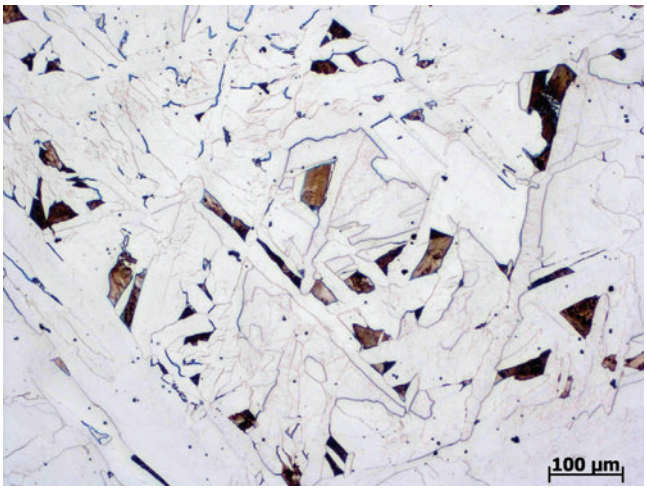

Figure 14. Micrograph of 1010 with 0.2% MM sample.

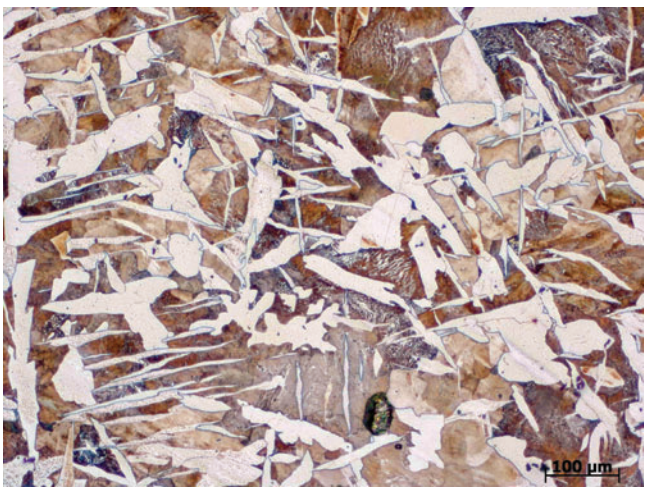

Figure 15. Micrograph of as-cast, baseline 1030 sample.

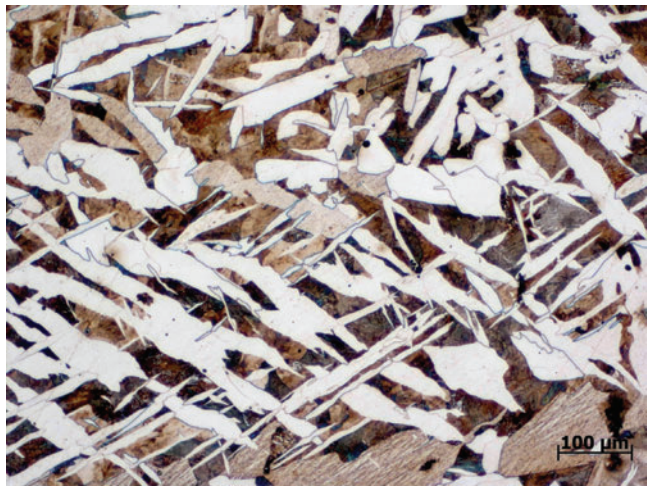

Figure 16. Micrograph of 1030 with 0.1% RS sample.

Figure 17. Micrograph of 1030 with 0.2% RS sample.

Figure 18 presents the microstructure of the 1030 sample with 0.1% misch metal. The free ferrite grain size is significantly smaller than the baseline 1030 material. The free ferrite also was more rounded. The reduction in grain size is consistent with a grain size reduction strengthening mechanism for this alloy. For the 1030 0.1% MM sample, the average yield strength was 296 MPa compared to 262 MPa for the baseline material.

Samples of the 1030 0.2% misch metal addition exhibited a fine grain structure and the highest strength (See Figure 9). The free ferrite had a significantly smaller grain size than the baseline material.

Electron Microscopy

An SEM with EDS was used to investigate the inclusions found in the rare earth-containing steels. Figure 20 depicts a typical oxide inclusion in the 1010 0.1% RE silicide sample. The gray region had a high RE content with about 11% aluminum. EDS analysis of the dark region indicated an aluminum-iron oxide with a small amount of cerium.

The inclusion depicted in Figure 21 from the 1010 0.2 % RE silicide sample contained an inner gray region with a combination of a high RE content and around 2% aluminum. This region also contained 8% sulfur. The dark region surrounding most of the inner gray region is an aluminum-iron oxide.

Figure 22 presents an inclusion in the 1010 0.1% misch metal sample. Many of the RE inclusions were rounded. The inclusion at the lower left has an inner light gray area surrounded by a darker gray. The light gray area consisted of a RE oxide with approximately 13% aluminum, while the darker gray area had a lower RE content and an aluminum level of 30%.

A common oxide inclusion for the 1010 0.2% misch metal sample is illustrated in Figure 23. The gray region has a high RE content with 11% aluminum. The dark region surrounding half of the inclusion consisted of an iron-aluminum oxide.

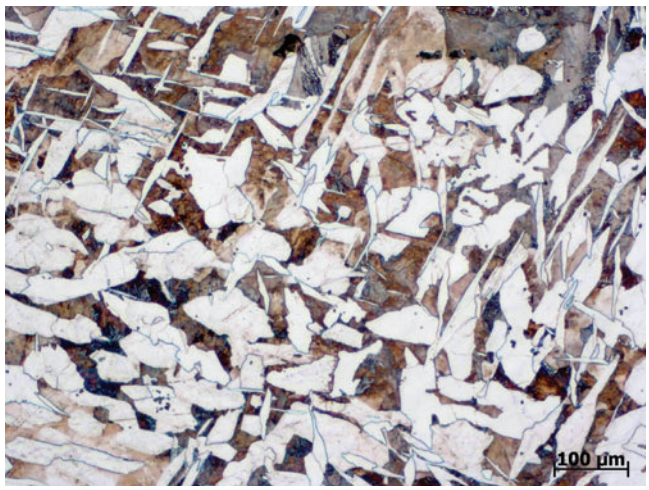

Figure 18. Micrograph of 1030 with 0.1% MM sample.

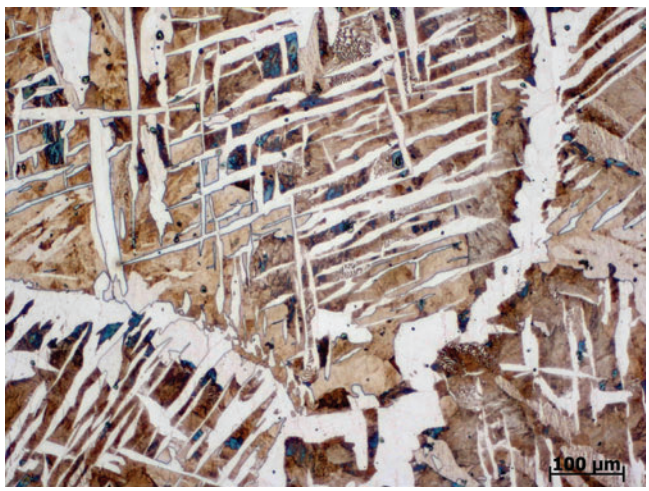

Figure 19. Micrograph of 1030 with 0.2% MM sample.

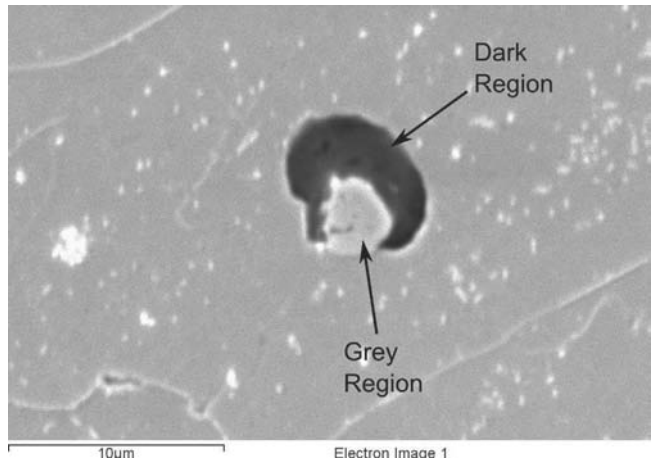

Figure 20. Image of a typical inclusion from the 1010 0.1% RS sample.

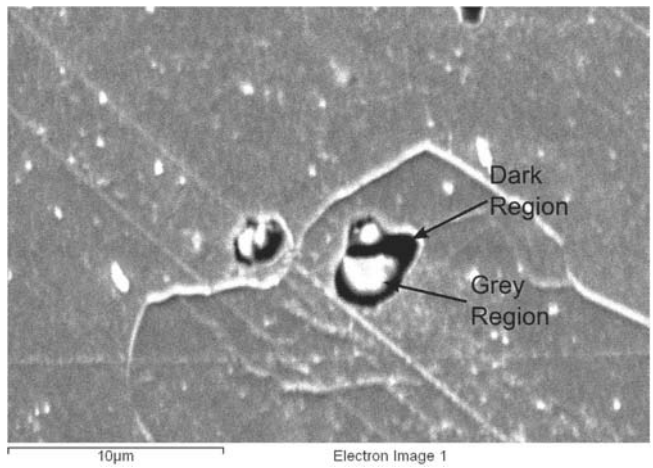

Figure 21 SEM image of oxides from the 1010 0.2% RS sample.

The 1010 0.1% RE silicide and 1010 0.2% misch metal samples contained a larger number of inclusions that were either not surrounded by another oxide or were only partially surrounded by another type of oxide. These encapsulating oxides were usually not high in RE. It is therefore likely that these slag coatings prevented the RE oxides that formed from acting as heterogeneous nuclei. This would explain the lower refinement and properties than the other samples.

The RE containing inclusions in the 1030 0.1% RE silicide sample appeared similar to some of the inclusions in the 1010 samples (Figure 24). At the gray center, the inclusions primarily consisted of a high RE content oxide with around 11% aluminum. Frequently, an iron-aluminum oxide partially surrounded these inclusions. Sometimes, these outer oxides contained significant levels of RE. The dark region surrounding the oxides in Figure 24 contained 10% RE.

Iron-aluminum oxides almost always encased the RE oxide inclusions in the 1030 0.2% RE silicide sample (Figure 25). The light gray inner portion usually contained a significant amount of RE and approximately 19% aluminum, while the dark outer encapsulating phase contained 13% RE elements.

Like the previous two samples, the RE inclusions had a gray inner region that was a RE rich oxide (Figure 26). These RE oxides contained around 10% aluminum. The outer dark region usually was an iron-aluminum oxide. However, in a few inclusions, this was an iron oxide with minor amounts of aluminum and RE elements. The encapsulating aluminum-iron or iron oxide did not fully surround all the RE oxides observed.

The 1030 0.2% misch metal addition sample contained RE inclusions similar to those observed in the previous samples. The gray center of these inclusions was usually a RE oxide (Figure 27). These oxides were frequently enveloped with a dark region of aluminum-iron or iron oxide. Not all of the inclusions were fully encapsulated, similar to the situation with the 1030 0.1% misch metal and 1030 0.1% RE silicide samples. All three of these samples had finer structures and higher yield strength than the baseline 1030 material.

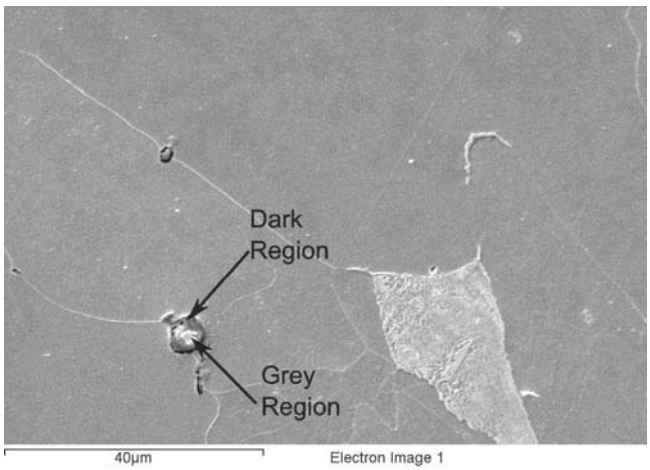

Figure 22. Typical incusion for the 1010 0.1%MM sample.

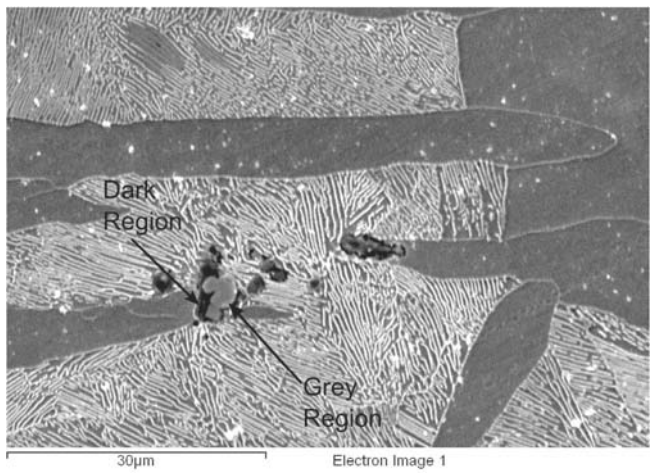

Figure 24. Electron micrograph of the 1030 0.1% RS sample.

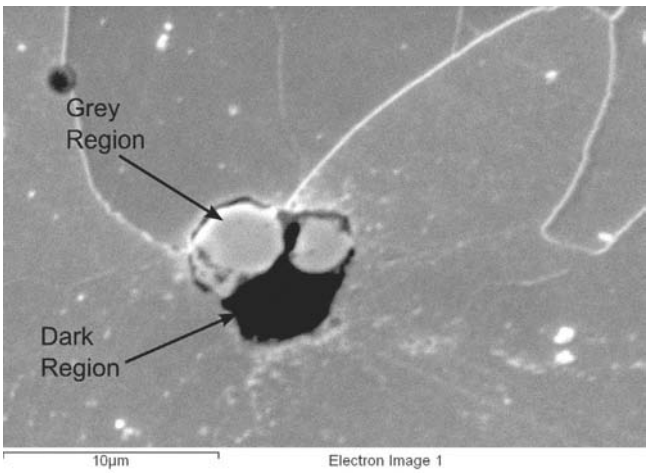

Figure 23. Electron micrograph of an inclusion in the 1010 0.2% MM sample

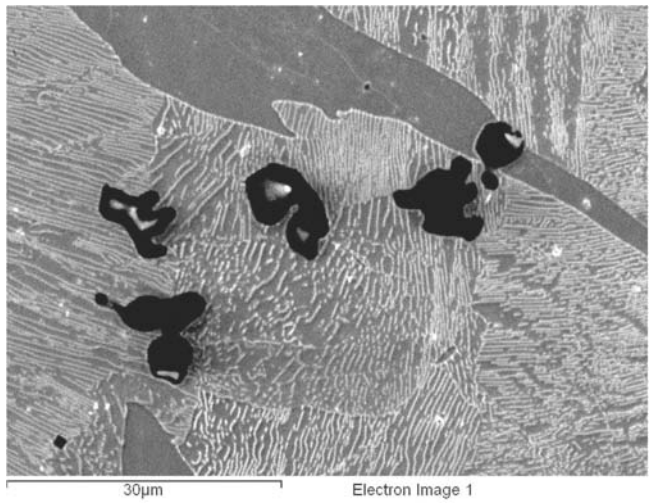

Figure 25. Typical inclusions for the 1030 0.2% RS sample.

Examination of the fracture surface in the 1010 bars found primarily dimple fracture. The samples contained large shrinkage pores within the gauge section (Figure 28). Many of the 1030 bars also had similar shrinkage defects (Figure 29). Even the bars with high elongation had pores on the same order of magnitude. The author cannot completely explain why these pores were so large. The plate casting design was designed using solidification modeling software to eliminate shrinkage porosity. Shrinkage of this magnitude is usually accurately predicted by this type of software. In any case, the high elongation in some of the 1010 samples despite these large defects was unexpected. Shrinkage porosity has been well documented as a cause of low ductility in cast metals.[14,18]

The electron microscopy observations indicate why there was not clear trend with addition alloy or TRE content. Samples with aluminum-iron oxide coatings on the RE oxides did not have finer microstructures or improved mechanical properties. The cause of these aluminum-iron oxides was likely reoxidation during tapping. Flow of the liquid during tapping was turbulent. The RE additions were added into the steel stream when it entered the ladle. These additions reacted with entrained oxygen to form RE oxides, but those same conditions appear to also randomly generate aluminum-iron oxides that either form on the outside of the RE oxide particles or coat the RE oxides later. These aluminum-iron oxides likely did not form during mold filling since computer mold filling simulations indicated a low velocity and laminar filling pattern. Also, the gating system controlled the in-gate velocity effectively. Less control had been exerted on the addition process because of human control of the furnace during tapping and human control of the exact point of RE additions. These variations could result in the inconsistent RE recovery observed and the seemingly random presence of the poisoning aluminum-iron oxide coating.

Strengthening Theory

Many of the authors working with RE additions have been working in austenitic stainless steels.[8,9,11] The austenitic steels experimented on were thought to solidify by forming primary austenite dendrites and never going through a solid

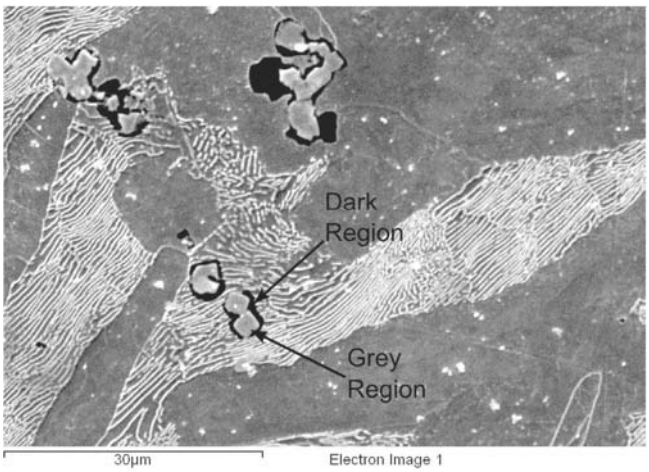

Figure 26. Electron micrograph of the 1030 0.1% MM sample.

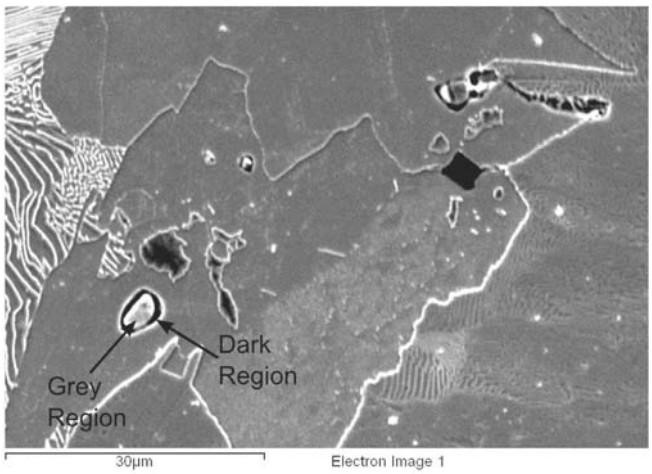

Figure 27. Image of typical inclusions from the 1030 0.2% MM sample.

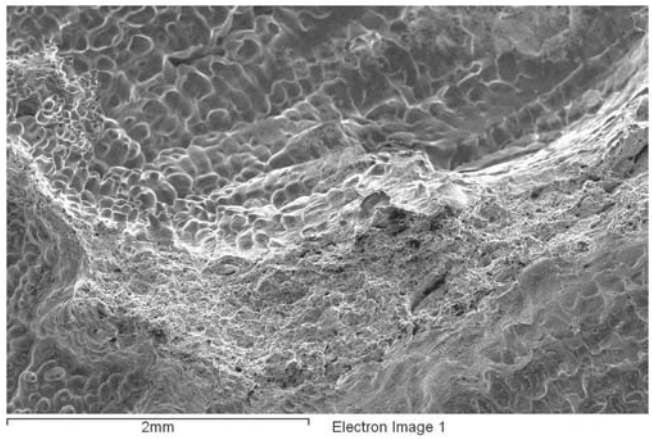

Figure 28. SEM image of large shrinkage pore in a 1010 tensile bar.

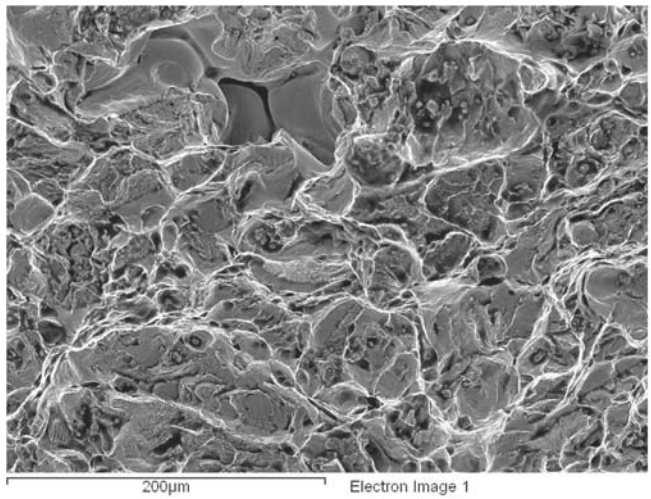

Figure 29. Fracture image for a 1030 sample.

state phase change to another crystal structure. Scheil calculations using the assumption that carbon diffuses quickly through the solid were conducted by the author using Thermo-Calc©. The experimental alloys in this work form δ-ferrite initially. For 1010 steel, the δ-ferrite phase was stable until approximately the last 3-5% of the solidification range, where it transformed to austenite. In the case of 1030 steel, the δ-ferrite was predicted to be the only phase formed for 50% of the freezing range. The remaining portion of the alloy solidified as austenite with the previous δ-ferrite transforming to austenite. This results in an inconsistency with the theories by other authors that RE oxides nucleate austenite in carbon steels.[6,7,19]

The microstructural observations in this work correlate with a heterogeneous-based grain refinement mechanism. In both alloys, heats with high RE content inclusions not completely surrounded by other oxides resulted in a finer overall structure. These finer grained alloys had higher yield strengths than the baseline material. If RE content primarily caused the reduction in observed grain size through a dendrite growth rate reducing mechanism, then the yield strength would be a direct function of TRE content. Since yield strength was not necessarily a function of TRE for both alloys, Li et. al's theory on dendrite growth inhibition due to RE element redistribution during solidification is not supported by the experimental observations in this research.[7]

Despite the evidence that rare earth particles play a significant role in reducing grain size, the theory that RE_2O_3 particles play the major role in heterogeneous nucleation is inconsistent with nucleation theory. The difference in lattice parameters between the crystal structure of these oxides and δ-ferrite are on the order of 20%, far higher than any observed heterogeneous nuclei.[1-5] The EDS results from this work indicated a TRE around 50-60% with 2-10% aluminum for the high RE content oxides. If RE_2O_3 oxides played the dominant role in assisting nucleation within these samples, then a composition closer to 85% TRE would be expected. A complicated oxide would be anticipated to have a different structure than the simple RE_2O_3 oxides theorized to nucleate austenite. Based on the evidence in this paper, the complex RE oxides found might have a structure capable of acting as a nuclei for δ-ferrite.

A second possible mechanism is the high RE content oxides did not play a major role in refining the as-cast structure but assisted the nucleation of austenite during the solid state transformation from δ-ferrite. The strong crystallographic matching between RE oxides and austenite would mean they could have acted as a solid state nuclei and assisted in the growth of austenite in the solid. This would result in increasing the number of austenite grains and create a finer grain size. Once the steel underwent the eutectoid reaction, the α-ferrite would have nucleated on the prior austenite grain boundaries, and a finer structure would be evident.

In either mechanism's case, the RE oxides would need an excellent crystallographic match to act as a nuclei. The aluminum-iron oxide coatings found in some of the samples with large grain sizes would prevent the RE oxides from being effective nuclei. This means both proposed mechanisms are consistent with the experimental observations from this research.

Future Work

A considerable amount of work remains to understand the role of heterogeneous nucleation in steels. A TEM study of the high RE content oxides would provide the necessary crystallographic information to determine their structure and confirm they act as heterogeneous nuclei. Further experimentation is necessary to determine how to ensure these RE oxides are not coated by another oxide. Such a development would improve the potency of RE additions and the mechanical properties of plain carbon steels.

The role of RE additions in stainless steels also would be of interest. Many stainless steels are not heat treatable, so an effective grain refining technique would improve their properties. Despite the work already done, the role of these additions are unclear. Additional experimentation on the structure-property relation in stainless steels with a RE addition would provide a dramatic improvement in the current understanding of their role in strengthening.

Conclusion

Rare earth additions were found to improve the yield strength of plain carbon steels. In several cases, the percent elongation of the 1010 samples with a RE addition also improved. The average yield strength of the 1010 samples with RE additions was 180 MPa compared to the 170 MPa average strength of the baseline 1010 samples. One set of samples had an average yield strength of 198 MPa. The samples with the highest strength had a finer grain size than the baseline 1010. This indicates the RE addition acted as a grain refiner. In the 1030 samples, the RE containing materials had an average yield strength of 288 MPa, significantly higher than the 262 MPa average yield strength for the 1030 baseline material. Again, the samples showing a finer microstructure had the highest yield strength.

Complex RE oxides were observed in the 1010 and 1030 materials. Some of the samples had RE oxides coated with an aluminum-iron oxide, which appears to prevent contact between the RE oxide and steel. The poisoning effect of this coating resulted in a grain size similar to the baseline material and, therefore, similar mechanical properties. This indicates the complex RE oxides acted as heterogeneous nuclei at some point in the microstructure development of the steels.

Acknowledgements

The author would like to acknowledge the financial support of the U.S. Navy's Office of Naval Research for supporting this work under award number N000140811052. Huron Casting provided additional support by machining and pulling the tensile bars. Special thanks to Lenard Noel and Jeremiah Winkle for their effort in conducting these experiments. Lastly, the author would like to thank Jennie Tuttle for her editorial assistance.

REFERENCES

1. Easton, M., St. John, D., "Grain Refinement of Aluminum Alloys: Part II. Confirmation of, and a Mechanism for, the Solute Paradigm," *Metallurgical and Materials Transactions A*, vol. 30A, pp. 1625-1633A (1999).
2. Kearns, M. A., Cooper, P. S., "Effects of Solutes on Grain Refinement of Selected Wrought Aluminum Alloys," *Materials Science and Technology*, vol. 13, no. 8, pp. 650-654 (1997).
3. Lee, Y. C., Dahle, A. K., St. John, D., "The Role of Solute in Grain Refinement of Magnesium," *Metallurgical and Materials Transactions A*, vol. 31A, no. 11, pp. 2895-2906 (2000).
4. Gruzleski, J. E., *Microstructure Development During Metalcasting*, p. 48, American Foundry Society, Schaumburg, IL (2000).
5. Bramfitt, B., "The Effect of Carbide and Nitride Addtions on the Heterogeneous Nucleation Behavior of Liquid Iron," *Metallurgical Transactions*, vol. 1, pp. 1987-1995 (1979).
6. Moore, J.J., "Rare Earth Desulphurisation of Sand Cast Steel, "*The British Foundryman*, vol. 75, no. 10, pp. 173-182 (1982).
7. Li, H., McLean, A., Rutter, J.W., and Sommerville, I.D., "Influence of Rare Earth Metals on the Nucleation and Solidification Behavior of Iron and 1045 Steel," *Metallurgical Transactions B*, vol. 19B, pp. 383-395 (1988).
8. Van der Eijk, C., and Walmsley, J., "Grain Refinement of Fully Austenitic Stainless Steels Using a Fe-Cr-Si-Ce Master Alloy," *Proceedings of the 59th Electric Furnace Conference*, pp. 51-60 (2001).
9. Suito, H., Ohta, H., and Morioka, S., "Refinement of Solidification Microstructure and Austenite Grain by Fine Inclusion Particles," *ISIJ International*, vol. 46, no. 6, p. 840-846 (2006).
10. Guo, M., and Suito, H., "Influence of Dissolved Cerium and Primary Inclusion Particles of Ce_2O_3 and CeS on Solidification Behavior of Fe-0.2 mass%C-0.02 mass%P Alloy," *ISIJ International*, vol. 39, no. 7, pp. 722-729 (1999).
11. Grong, O., Kolbeinsen, L., Eijk, C., and Tranell, G., "Microstructure Control of Steels through Dispersoid Metallurgy Using Novel Grain Refining Alloys," *ISIJ International*, vol. 46, no. 6, pp. 824-831 (2006).
12. Lan, J., Junjie, H., Wenjiang, D., Qudong, W., and Yanping, Z., "Effect of Rare Earth Metals on the Microstructure and Impact Thoughness of a Cast 0.4C-1.2Mo-1.0V Steel," *ISIJ International*, vol. 40, no. 12, pp. 1275-1282 (2000).
13. Campbell, J., *Castings 2nd Ed.*, p 280, Elsevier Butterworth-Heinemann, Burlington, MA (2004).
14. Gruzleski, J. E., Closset, B. M., *The Treatment of Liquid Aluminum-Silicon Alloys*, p 140, American Foundry Society, Schaumburg, IL (1990).
15. Jorstad, J. L., Rasmussen, W. M., *Aluminum Casting Technology*, p. 29, American Foundry Society, Schaumburg, IL (2006).
16. Makarov, A. V., Savrai, R. A., Schastivtsev, V. M., Tabatchikova, T. I., Egorova, L. Y., "Mechanical Properties and Fracture upon Static Tension of High-Carbon Steel with Different Types of Pearlite Structure," *The Physics of Metals and Metallography*, vol. 104, no. 5, pp. 522-534 (2007).
17. Taleff, E. M., Syn, C. K., Lesuer, D. R., Sherby, O. D., "Pearlite in Ultrahigh Carbon Steels: Heat Treatments and Mechanical Properties," *Metallurgical and Materials Transactions A*, vol. 27A, no. 1, pp. 111-118 (1996).
18. Qingxian, Y., Xuejun, R., Bo, L. Mej, Y., "Discussion of RE Inclusions as Heterogeneous Nuclei of Primary Austenite in Hardfacing Metals of Medium-High Carbon Steels," *Journal of Rare Earths*, vol. 17, no. 4, pp. 293-297 (1999).
19. Moore, J. J., Hebsur, M. G., Ravipati, D. P, Arnson, H., "In Mold Rare Earth Treatment of Cast Steel," *Transactions of the American Foundrymen's Society*, vol. 91, pp. 433-444 (1983).

Effect of Rare Earth Additions on Grain Refinement of Plain Carbon Steels

R. Tuttle, Department of Mechanical Engineering, Saginaw Valley State University, University Center, MI USA

Reviewer: It is also not clear that the effect of the additives is nucleation of delta ferrite, and not in their effect on subsequent phase transformation. Please comment on this.

Author: *While other researchers have concluded that rare earth (RE) oxides must assist the nucleation of delta ferrite due to their own observations of grain size reduction, there is a discrepancy in this theory. Crystallographic matching between delta ferrite and RE oxides is high enough that the author questions the validity of such a theory. The author contemplated that perhaps the presence of RE oxides made the initiation of austenite dendrites easier because there was a nucleation site for them. A similar situation exists in cast irons where inoculants are added to assist the growth of graphite instead of cementite. However, no experimental evidence from this work or his other work supported such an idea so this explanation was not included in the text. Another possible route is that the RE oxides act as nuclei during the transformation from delta ferrite to austenite during the solid state transformation. Creating more austenite grains would cause a reduction in the austenite grain size which would then result in a reduction in the alpha ferrite grain size in the final room temperature microstructure. The revised paper includes information regarding this second mechanism and incorporates this new literature source.*

Reviewer: The author inspects the room temperature grain size that may bear little relation to the as-solidified grain size that he appears to be targeting in the effort to produce grain refinement. The room temperature grain size has suffered at least one or two solid state phase changes when cooling from the freezing temperature.

Author: *The reviewer is correct that there is some trouble with examining room temperature grain size as a proxy for the as-cast grain size. These steels go through one or two solid state transformations before the room temperature microstructure develops. However, the solid state transformations initiate at the existing grain boundaries and move inwards as they progress. The result is that they initiate at the grain boundaries of the decomposing phase. Therefore, final grain size is dependent on the initial grain size as long as the steels being compared have similar thermal histories. This is why the castings were always allowed to cool in the mold until they were below the eutectoid temperature and no additional heat treatments were done. It was vital for any useful comparisons that every test casting had a similar cooling history. None of the samples from this series of experiments responded to the picric acid etchant that was etchant to reveal the prior austenite grain boundaries. Etching for prior austenite grain boundaries can be difficult to successfully complete. The literature has several references to the random ineffectiveness of the various prior austenite etching procedures for some alloys. Other researchers have indicated that steels of the same grade can exhibit drastically different etching behavior when trying to determine prior austenite structure. Also, since these alloys should initially solidify as delta ferrite such etching would still not give a precise picture of the as-cast structure.*

Some researchers have used high phosphorous levels to determine the delta ferrite structure. This technique works because the phosphorous strongly segregates during solidification. On subsequent etching, the high phosphorous regions that correspond to the interdendritic liquid at the final stages of solidification etch differently than the other portions of the steel. This provides great contrast. The problem with this approach is that the mechanical properties are detrimentally impacted by the high phosphorous levels. Comparisons to any commercial material would not be possible by readers. The author thought that it was better to use a steel composition closer to commercial alloys to help industrial readers of his work interpret the commercial implications. In the next phase of this grain refining project, the author is strongly thinking about using this approach to better understand how the as-cast structure develops and is related to the final structure.

Reviewer: The test casting design appears lacking in that it will allow entrapment of oxides from the melt and oxides generated during pouring into the area of the casting from which the test bars are pulled. If oxides are present in the metal, is that reflected in the mechanical properties of the test specimens? Does the appearance of shrinkage porosity confirm the oxides in the metal and the poor ductility results? The ductility properties are low especially for 1030; those that are higher are merely approaching the values to be expected (all values should be in the range 30 to 50% elongation). The large feeder on the casting was carefully checked by computer simulation and should have been sufficient to prevent shrinkage porosity. Is the observed porosity truly shrinkage? The oxides generated from the current filling system could overwhelm all other aspects of this work. This should be addressed.

Author: *The gating system for the casting follows standard filling system design and was also verified by computer simulation. A gating ratio of 1:4:4 was used to maintain low metal velocities. Simulation predicted a maximum velocity in the in-gate of 0.5 m/s. Metal velocities were far lower inside the part cavity. These lower velocities reduce the turbulence while filling the mold and prevent entrainment of re-oxidation products. Observation of the filling*

during the experiments demonstrated a filling pattern very close to the computer simulations. The only improvement to the gating system would be the use of a filter. A filter would certainly ensure that any oxides or slag from the pouring ladle would not enter the casting. However, it would also have a tendency to remove the La_2O_3 powder added during pouring. Since the author was testing the addition of these powders into the steel, it would have negated one aspect of the research being conducted.

Microstructural examination of the castings found a lower inclusion content than the author has observed in industrial castings, a direct result of the gating system employed. Also, oxides were not usually observed with the shrinkage porosity in the fracture surfaces. The addition of rare earth elements should have actually made the number and severity of oxides within the castings with RE additions worse than the baseline material. As such, one would expect that all of the mechanical properties were worse than the baseline. That was not observed in the data.

There was a clear difference in the final microstructures for some of the castings due to the addition of RE elements. Electron microscopy investigation also found a reason why RE additions worked in some cases and not in others. Therefore, much can be learned about the nucleation events in steel castings through this study.

Reviewer: The author should take account of the new theories of the design of molds and casting systems. Using inappropriate designs, such as the use of a conical pouring basin (assumed since no design was given), a well at the base of the sprue, together with the 1:4:4 gating ratio is not recommended. The damage to the castings is confirmed, by among other things, the poor elongation results and their extreme scatter. Furthermore, there appears to be no discernible effect of the addition of the rare earth oxide powder. Any minor effect is swamped by the scatter, putting the results of the research in question.

Author: *As stated, the gating system used in the test casting represents good steel casting practice of the industry. It is common to use a sprue well and a gating ratio of 1:2:2 in steels. The 1:4:4 ratio was chosen to provide a slower fill rate to reduce oxide entrainment and re-oxidation of the steel. Newer theories on gating system design are far from universally accepted. The use of computer simulations provides a better tool for evaluating the overall effectiveness of gating systems. Regarding elongation, significant scatter in elongation data can be caused by the testing method used. The company that conducted the tensile test uses extensometer data for calculating percent elongation. If the extensometer slips during the tensile test, this can lead to significant errors in the elongation measurement during fracture. It is better practice to measure elongation using gauge marks on the specimens. Unfortunately, the company providing the testing does not have the appropriate indenting fixture. It seems to the author that it is far more likely that the errors in measuring the elongation are causing the variation observed in the data than the presence of oxides or bi-films.*

Reviewer: Table two seems to be shows a lot of variability in TRE content when the same type and amount of additions are made. This variability could explain some of the erratic results.

Author: *Rare earth recovery varied significantly during the tests. Researchers actually repeated several of the experimental treatments in an attempt to obtain the same TRE values. Discussions with a set of European researchers that have used rare earth oxide additions in stainless steel have indicated that they have also observed the same problem. It appears the in-stream addition during tapping results in significant and variable rare earth losses. The most likely cause are differences in how the steel stream impacts the ladle during filling and exactly how the rare earth containing pieces hit the stream. The author currently has work examining how to eliminate this variability by changing the addition method. This variation in TRE content is why yield strength was plotted as a function of actual TRE content to assist in examining the actual factors involved.*

As also pointed out in the paper, many of the RE oxides in the poorly performing RE added steels had a reoxidation coating. This coating would prevent the RE oxides from acting as nuclei regardless of the TRE content of the alloy. Without direct contact between the steel and RE oxides there is no way for the RE oxides to assist any phase reactions. This factor and the variable rare earth recovery likely explain the lack of improvement for these alloys.